Title

Heterologous production of 1-tuberculosinyladenosine in *Mycobacterium kansasii* models pathoevolution towards the transcellular lifestyle of *Mycobacterium tuberculosis*.

Authors

Marwan Ghanem[1,2,3,4]*, Jean-Yves Dubé[1,2,3]*, Joyce Wang[1,2,3,5], Fiona McIntosh[1,2,3], Daniel Houle[2], Pilar Domenech[1,2,3], Michael B. Reed[1,2,3], Sahadevan Raman[6], Jeffrey Buter[7], Adriaan J. Minnaard[7], D. Branch Moody[6] and Marcel A. Behr[1,2,3]

Affiliations

1. Department of Microbiology and Immunology, Faculty of Medicine, McGill University, Montreal, Canada. 2. Infectious Disease and Immunity in Global Health Program, Research Institute of the McGill University Health Centre, Montreal, Canada. 3. McGill International TB Centre, Montreal, Canada. 4. Faculty of Medicine, American University of Beirut, Lebanon. 5. Department of Microbiology and Immunology, University of Michigan Medical School, Michigan, USA. 6. Division of Rheumatology, Immunity and Inflammation, Brigham and Women's Hospital, Harvard Medical School, Boston, United States of America. 7. Stratingh Institute for Chemistry, University of Groningen, 9747AG Groningen, The Netherlands. *These authors contributed equally.

Running title: 1-TbAd complementation in *M. kansasii*

Author for correspondence: Marcel Behr (marcel.behr@mcgill.ca)

25 **Byline:** Ghanem M*, Dube JY*, Wang J, McIntosh F, Houle D, Domenech P, Reed MB, Raman S,
26 Buter J, Minnaard AJ, Moody DB and Behr MA. 2020. Heterologous production of 1-
27 tuberculosinyladenosine in *Mycobacterium kansasii* models pathoevolution towards the
28 transcellular lifestyle of *Mycobacterium tuberculosis*.
29

30 **ABSTRACT**

31 *Mycobacterium kansasii* is an environmental non-tuberculous mycobacterium that
32 causes opportunistic tuberculosis-like disease. It is one of the most closely related species to the
33 *M. tuberculosis* complex. Using *M. kansasii* as a proxy for the *M. kansasii*-*M. tuberculosis*-
34 common ancestor, we asked whether introducing the *M. tuberculosis*-specific gene pair *Rv3377c*-
35 *Rv3378c* into *M. kansasii* affects the course of experimental infection. Expression of these genes
36 resulted in the production of an adenosine-linked lipid species, known as 1-
37 tuberculosinyladenosine (1-TbAd), but did not alter growth *in vitro* under standard conditions.
38 Production of 1-TbAd enhanced growth of *M. kansasii* under acidic conditions through a bacterial
39 cell-intrinsic mechanism independent of controlling pH in the bulk extracellular and intracellular
40 spaces. Production of 1-TbAd led to greater burden of *M. kansasii* in the lung of C57Bl/6 mice
41 during the first 24 hours after infection and *ex vivo* infections of alveolar macrophages
42 recapitulated this phenotype within the same time frame. However, in long-term infections,
43 production of 1-TbAd resulted in impaired bacterial survival in both C57Bl/6 mice and *Ccr2*-/-
44 mice. We have demonstrated that *M. kansasii* is a valid surrogate of *M. tuberculosis* to study
45 virulence factors acquired by the latter organism, yet shown the challenge inherent to studying
46 the complex evolution of mycobacterial pathogenicity with isolated gene complementation.

47

48 **IMPORTANCE**

49 This work sheds light on the role of the lipid 1-tuberculosinyladenosine in the evolution
50 of an environmental ancestor to *M. tuberculosis*. On a larger scale, it reinforces the importance
51 of horizontal gene transfer in bacterial evolution and examines novel models and methods to
52 provide a better understanding of the subtle effects of individual *M. tuberculosis*-specific
53 virulence factors in infection settings that are relevant to the pathogen.

54

55 **INTRODUCTION**

56 *M. tuberculosis* virulence factors have been established by genetic knock-out and
57 complementation within the pathogen, producing evidence of an attenuation of virulence in *ex*
58 *vivo* or *in vivo* experimental infections (1, 2). While numerous virulence-associated loci have been
59 identified with this approach, the majority of these are intact in the genomes of non-
60 transmissible environmental mycobacteria, such as *M. kansasii* (3-6). *M. kansasii* is readily
61 isolated in clinical settings from pulmonary infections and we have previously shown that it can
62 be studied in an experimental lung model (3). However, although it causes TB-like disease, *M.*
63 *kansasii* infections disproportionately affect patients with underlying pulmonary diseases or
64 immunosuppression, and there is no evidence supporting its transmission between individuals
65 (7, 8). The conservation of many virulence factors across *M. tuberculosis* and *M. kansasii*,
66 including the ESX-1 secretion system, PhoPR 2-component system and DosR/S/T regulon suggest
67 that they play a role in a broader survival strategy used by mycobacteria (9-11). For example,
68 some of these factors may be needed for survival of *M. kansasii* within free-living phagocytic

69 amoeba, but their presence does not provide *M. kansasii* with the pathogenic capabilities of *M.*
70 *tuberculosis* inside human hosts (12). Consequently, there is currently an incomplete
71 understanding of how *M. tuberculosis* emerged as a human-adapted professional pathogen.
72
73 It was previously thought that horizontal gene transfer (HGT) does not occur in
74 mycobacteria. However, evidence accumulated over the past decade has shown that HGT events
75 have happened during mycobacterial speciation and are associated with the step-wise
76 emergence of pathogenic species (13-16). Fifty-five genes have been acquired by *M. tuberculosis*
77 since its divergence from the *M. kansasii*-*M. tuberculosis* common ancestor (MKMTCA) (13).
78 Although many of these HGT genes have no postulated function, the *Rv3376*-*Rv3378c* genomic
79 island uniquely present in *M. tuberculosis* is known to encode a class II terpene cyclase (*Rv3377c*)
80 and a tuberculosinyl transferase (*Rv3378c*). Together, the two enzymes are responsible for the
81 conversion of geranylgeranyl pyrophosphate (GGPP) into the recently identified *M. tuberculosis*-
82 specific lipid 1-tuberculosinyladenosine (1-TbAd), which is a potential diagnostic molecular
83 marker for TB disease (17-20). 1-TbAd further undergoes a chemical rearrangement, known as
84 the Dimroth reaction, to generate N^6-TbAd (18). While GGPP is found in both species and used
85 as an intermediate in the biosynthesis of 1-TbAd by *M. tuberculosis* (17, 19), it is part of the
86 biosynthetic pathway for the production of carotenoid pigments of *M. kansasii*, giving its
87 characteristic yellow colour (21).
88
89 We previously reported the important role of 1-TbAd in protecting *M. tuberculosis* from
90 phagosomal acidification inside macrophages (22). In the present work, we have characterized

91 the effect of 1-TbAd production in *M. kansasii* complemented with *Rv3377c and Rv3378c*. Here,
92 we show that *in vitro* growth kinetics and colony morphology in liquid and on solid media are
93 unaltered by *Rv3377c-Rv3378c* expression. 1-TbAd confers a growth advantage in acidic media
94 compared to wild-type *M. kansasii*, which we further demonstrated to be independent of
95 cytosolic and culture medium pH control, suggesting a compartmental mechanism of protection
96 for the bacterium. *Rv3377c-Rv3378c* provided an early advantage to bacterial replication during
97 pulmonary infection in mice, consistent with enhanced survival in alveolar macrophages.
98 However, the *M. kansasii:Rv3377-78c* was outcompeted by the wild-type during long-term
99 murine infection. This study demonstrates that we can use *M. kansasii* as a proxy of the MKMTCA
100 to explore the complex evolution of *M. tuberculosis*. It also shows that gene acquisition likely
101 provided advantages for specific contexts, including a possible and unexpected role in survival
102 within alveolar macrophages during early stages of infection, despite tradeoffs or challenges
103 under other circumstances requiring further evolution to overcome.
104

105 **RESULTS**

106 **Expression of *Rv3377c-Rv3378c* in *M. kansasii* leads to 1-TbAd production**

107 We introduced the *M. tuberculosis*-specific gene pair *Rv3377c-Rv3378c* into the *M.*
108 *kansasii* genome within an integrative plasmid containing hygromycin resistance to produce *M.*
109 *kansasii::Rv3377-78c* (see methods). As a control for subsequent experiments, an integrative
110 'empty vector' (EV) was employed. After labelling with ^{14}C-adenosine and lipid extraction using
111 chloroform and methanol, radio-thin-layer chromatography (TLC) was used to detect adenosine-
112 linked lipids in *M. kansasii:Rv3377-78c* clones for comparison to *M. tuberculosis* strain H37Rv

113 (Fig. 1a). Conventional molybdenum-based sprays followed by charring broadly detected all lipids
114 as a loading control (Fig. 1b). Whereas uncomplemented bacterial extracts showed material at
115 the origin and one weak band in radio-TLC, *Rv3377c-Rv3378c* complementation generated at
116 least 5 additional lipid species. Three of these novel lipids co-migrated with compounds from *M.*
117 *tuberculosis* strain H37Rv. Both results strongly suggested the successful genetic transfer of *M.*
118 *tuberculosis*-associated adenosine-linked lipids to *M. kansasii.* 5% phosphomolybdic acid reagent
119 (PMA) staining showed that similar amounts of total lipids were spotted for each *M. kansasii*
120 sample (Fig. 1b).
121
122 High-performance liquid chromatography-mass spectrometry (HPLC-MS) was used to
123 chemically identify the compounds produced by *M. kansasii::Rv3377-78c*, in which the expected
124 retention of 1-TbAd (22.7 min) and N^6-TbAd (5.8 min) were known (Fig. 1c-g). Whereas the *M.*
125 *kansasii*::EV control did not release compounds that comigrated with either 1-TbAd or N^6-TbAd,
126 *M. kansasii:Rv3377-78c* produced high intensity (6.7-7.0 x10^6 counts) signals (*m/z* 540.354)
127 matching the expected retention time and mass (*m/z* 540.3544) of the proton adducts of 1-TbAd
128 and N^6-TbAd. The extractions were performed at a range of pH (4.5 – 7.4) since both the Dimroth
129 reaction that generates N^6-TbAd and the capture of lysosomotropic agents are sensitive to pH,
130 as previously explained (18, 22, 23). However, there was no clear impact of altering pre-
131 extraction pH for two hours to the release nor relative abundance of 1-TbAd and N^6-TbAd,
132 suggesting that such effects, if existent, did not occur under the tested conditions (Fig. 1c-g).
133 Similar to patterns observed from *M. tuberculosis*, more 1-TbAd than N^6-TbAd was recovered
134 from *M. kansasii*::*Rv3377-78c* (Fig. 1f-g).

135

136 **1-TbAd production does not change visible characteristics of *M. kansasii* in conventional media**

137 To characterize any overt phenotypic effects of 1-TbAd production on *M. kansasii*, we
138 assessed its influence on *in vitro* characteristics of the bacterial culture. *M. kansasii*::*Rv3377-78c*
139 grew similarly to wild-type *M. kansasii* and *M. kansasii*::EV in 7H9 (Fig. 2a) and on 7H10 agar (Fig.
140 2b). Since the production of 1-TbAd requires the same intermediate GGPP as that of the yellow
141 pigment that *M. kansasii* produces when exposed to light, we then tested *M. kansasii*::*Rv3377-*
142 *78c*'s ability to turn yellow after light exposure in order to rule out the possibility that a pigment-
143 related phenomenon might affect our outcomes (Fig. 2b). *M. kansasii*::*Rv3377-78c* retained
144 photochromogenic abilities by turning yellow after exposure to light at room temperature within
145 the same timeframe as *M. kansasii*::EV.

146

147 Congo Red is an amphiphilic dye that binds to the mycobacterial cell membrane. When
148 grown on Congo Red-containing 7H10 plates, different mycobacteria retain the dye distinctly,
149 and this feature has been associated with differences in the interactions of bacterial cells within
150 the colony (24). In this study, *M. tuberculosis* absorbed the dye and became red, while *M. kansasii*
151 colonies remained white on the plate. Since 1-TbAd is found on the cell surface and has an
152 amphipathic character (17), we tested the effect of its production on intra-colony bacterial
153 interactions of *M. kansasii*::*Rv3377-78c*. Visual inspection of colonies (Fig. 2c) and absorbance at
154 488nm (Fig. 2d) showed no difference in retention of Congo Red between *M. kansasii*::EV and *M.*
155 *kansasii*::*Rv3377-78c*.

156

157 **1-TbAd production enhances growth of *M. kansasii* in acidic media**

158 The ability to survive in mildly acidic environments is a key feature of mycobacteria, both
159 environmental and pathogenic (25, 26). It was recently shown that 1-TbAd production in *M.*
160 *tuberculosis* confers a growth advantage over a pH range (5.0-5.4) comparable to that of an
161 activated phagolysosome, which is not tolerated by most bacteria (22). To confirm whether 1-
162 TbAd production provides protection to *M. kansasii* in acidic 7H9 broth, we inoculated *M.*
163 *kansasii*::EV or *M. kansasii*::*Rv3377-78c* into fresh pH-adjusted 7H9 media (pH 4.9, 5.0, 5.1, 5.2,
164 5.4, 6.6) and monitored their growth. As expected, *M. kansasii*::*Rv3377-78c* was able to grow in
165 lower pH than *M. kansasii*::EV (Fig. 3a). This effect was observed consistently in five experiments
166 with a growth differential observed between pH 5.1 and 5.4. In addition, as 1-TbAd can be shed
167 extracellularly to de-acidify the phagosomal environment as seen in *M. tuberculosis*, we
168 hypothesized that the production of 1-TbAd by *M. kansasii::Rv3377-78c* may modulate media pH
169 (22). However, at 8 and 17 days post inoculation, both *M. kansasii*::EV and *M.kansasii::Rv3377-*
170 *78c* slightly increased the pH of the media where there was bacterial growth, and to a similar
171 extent (Fig. 3b). Therefore, although we observed enhanced growth with *M. kansasii::Rv3377-*
172 *78c* compared to *M. kansasii*::EV, we could not demonstrate a causative role for 1-TbAd raising
173 the extracellular pH of the culture media under these conditions.

174

175 **Synthetic 1-TbAd does not directly enhance growth of *M. kansasii***

176 Prior work with *M. tuberculosis* estimated that 1-TbAd might naturally accumulate to μM
177 concentrations in phagosomes, and 5-20 μM 1-TbAd alters lysosomal pH and morphology in
178 human macrophages (22). The proposed lysosomotropic mechanism requires that 1-TbAd access

179 a low pH compartment where the uncharged conjugate base binds protons to raise pH and
180 regenerate a concentration gradient that promotes further entry of uncharged conjugate base
181 to the acidic compartment. Whereas this mechanism can relieve pH stress on the bacterium, the
182 major alternative, which is not exclusive of lysosomotropism, is that 1-TbAd directly signals for
183 bacterial growth and division. To distinguish these mechanisms we 'chemically complemented'
184 WT *M. kanasii* with synthetic 1-TbAd and N^6-TbAd added externally in media. In this experiment
185 TbAd (already carrying a proton) should not alter pH, but would contact bacteria in high
186 concentrations. As expected the addition of synthetic 1-TbAd (pK_a ~ 8.5) and N^6-TbAd (pK_a ~ 3.8)
187 did not alter the pH of the 7H9 media (Sup. Fig. 1a). Next we inoculated *M. kansasii* into pH-
188 adjusted 7H9 broth (pH 4.0, 4.8, 5.0, 5.2, 5.4, 6.7,) containing 1, 5, 10 or 20 μM TbAd and
189 monitored growth over 16 days (Fig. 4 and Sup. Fig. 1b). With increasing doses of 1-TbAd or its
190 isomer N^6-TbAd, we did not observe any promotion of *M. kansasii* growth in normal nor acidic
191 7H9 broth (Fig. 4 and Sup. Fig 1b). In fact, 1-TbAd partially inhibited growth at 20 μM, the highest
192 dose tested, at normal pH. These data demonstrated that the protection from low pH in 7H9
193 culture media afforded by *Rv3377c-Rv3378c* complementation in *M. kansasii* is cell-intrinsic,
194 promotes growth only at low pH and does not occur with direct exposure to protonated TbAd.
195

196 **1-TbAd does not maintain bulk cytosolic pH to enhance *M. kansasii* growth in low pH media**

197 We aimed to identify whether 1-TbAd production alters/maintains the pH of the bacterial
198 cytosol when grown in acidic media. *M. kansasii*::EV or *M.kansasii::Rv3377-78c* were stained
199 with CFSE to measure their intracellular pH while monitoring their growth in different pH-
200 adjusted 7H9 broth (pH 4.0, 4.8, 5.0, 5.2, 5.4, 6.0, 6.7, 7.2) overnight (Fig. 5). Lower initial pH of

201 the media was associated with lowering intracellular pH over the experimental timeframe, as
202 expected. Importantly, we observed the expected growth advantage with 1-TbAd production at
203 lower pH (5.0), but there was no apparent intracellular pH difference between *M. kansasii* strains
204 at this or any pH. Thus, 1-TbAd production does not aid *M. kansasii* growth at low pH by
205 maintaining the pH of the bulk intracellular milieu, suggesting the growth advantage is provided
206 by countering the effect of low pH in a specific region of the cell.
207
208 **1-TbAd production enhances establishment of *M. kansasii* lung infection and survival in**
209 **alveolar macrophages.**
210 1-TbAd is hypothesized to promote virulence of *M. tuberculosis* by countering phagosome
211 acidification, enhancing survival of the pathogen *in cellulo* (19, 27, 28). We therefore wished to
212 test the virulence of *M. kansasii*::*Rv3377-78c.* In C57Bl/6 mice, *M. tuberculosis* expands in a
213 logarithmic scale within the early course of infection. In sharp contrast, *M. kansasii* remains at its
214 initial levels of infection, suggesting it is a good model for acquisition-of-virulence studies within
215 the mouse (3). As a measure of virulence, we hypothesized that the pulmonary bacterial load of
216 *M. kansasii* in mice would be enhanced with 1-TbAd production. During pilot experiments, we
217 infected mice with *M. kansasii*::EV and *M. kansasii*::*Rv3377-78c* through aerosolization, and
218 infections with either strain resulted in a pulmonary burden within one log of the initial infection
219 up to day 42, with no clear differences between both groups (Sup Fig. 2).
220
221 Despite repeated attempts to standardize the inoculum, we consistently noted a higher
222 number of 1-TbAd-producing *M. kansasii::Rv3377-78c* one day after aerosol infection when

223 compared with *M. kansasii*::EV (not shown). To test if *Rv3377c-Rv3378c* was altering the dose
224 administered or instead enhancing establishment or early growth, mice were aerosolized with
225 *M. kansasii*::EV or *M. kansasii*::*Rv3377-78c* and their lungs were collected and homogenized
226 shortly (4 hours) after infection and compared to bacterial counts 24 hours after infection (Fig.
227 6a-b). Equivalent 4-hour CFU counts were observed for *M. kansasii*::EV and *M. kansasii*::*Rv3377-*
228 *78c*; only the latter multiplied successfully 24 hours later (Fig. 6a). *M. kansasii*::*Rv3377-78c*
229 showed a 1.5-fold increase in numbers from 4 to 24 hours while *M. kansasii*::EV numbers
230 remained equal (Fig. 6b). The experiment was performed three times, once at a low dose of 100
231 CFUs/lung and twice at a higher dose of 750 CFU/lung, with *M. kansasii*::*Rv3377-78c* consistently
232 attaining larger numbers by 24 hours post-infection in all three instances (Sup. Fig. 3).
233
234 We hypothesized that 1-TbAd was enhancing proliferation of *M. kansasii* in the lungs by
235 promoting survival in resident macrophages. First, using bone marrow-derived macrophages
236 (BMDMs), we infected with *M. kansasii*::EV or *M. kansasii*::*Rv3377-78c* and collected cell lysates
237 at 4- and 24-hours post infection: the infections proceeded similarly with both bacteria unlike
238 what we had observed in mouse lungs *in vivo* (Sup. Fig. 4). Alveolar macrophages (AMs) are
239 resident lung macrophages that phagocytose infectious agents entering the lower airways (29).
240 We assessed whether fitness would be altered in an *ex vivo* infection of murine AMs. In two
241 independent experiments, *M. kansasii*::*Rv3377-78c* increased in numbers by CFU counts from 4
242 to 24 hours post infection, while *M. kansasii*::EV numbers were largely unchanged and inferior
243 to *M. kansasii*::*Rv3377-78c* after 24 hours (fig. 6c-d). *M. kansasii*::*Rv3377-78c* exhibited a 2.0-fold
244 increase compared to the 1.1-fold increase seen in *M. kansasii*::EV (Fig. 6e). This is consistent

245 with our observations in murine lungs and with the conclusion that 1-TbAd provides an advantage
246 to *M. kansasii* during the early stages of pulmonary infection by specifically promoting survival
247 or growth in resident alveolar macrophages.
248
249 **1-TbAd production impairs long-term persistence during mixed lung infections**
250 We validated a translaryngeal infection model wherein WT *M. kansasii* was directly
251 introduced into the upper respiratory tract (Sup. Fig. 5 and methods) (30). Mice were monitored
252 for 42 days; bacteria persisted at the same log CFU as the initial infection and the mice did not
253 become overtly sick (Sup. Fig. 5). To test the effect of 1-TbAd in a high-dose competitive infection,
254 we used the translaryngeal infection model to generate a mixed infection with $3x10^6$ CFUs of a
255 1:1 WT *M. kansasii* and *M. kansasii*::*Rv3377-78c* (Fig. 7a). Lung homogenates plated on 7H10
256 plates with and without 50 µg/ml hygromycin revealed a statistically significant decrease in the
257 *M. kansasii*::*Rv3377-78c* to WT *M. kansasii* ratio over time, with an initial decrease in the
258 proportion of *M. kansasii*::*Rv3377-78c* in the bacterial population from 0.48 (week 0) to 0.27
259 (week 1), stabilizing at that latter proportion over time (Fig. 7a). The competitive setting was
260 established to identify more subtle effects that the production of 1-TbAd could have on the
261 producing cells or the whole bacterial population over time. These findings show that such a
262 beneficial effect does not exist in the tested settings.
263
264 C-C chemokine receptor 2 (CCR2) is an essential component for defense in the airways;
265 *Ccr2-/-* mice lose the ability to recruit non-tissue resident immune cells and succumb to *M.*
266 *tuberculosis* infection (31). We used these mice to test whether the short-term AM phenotype

267 could be recapitulated in a longer-term *in vivo* setting without the interference of recruited
268 immune cells in WT mice that might explain the lack of a phenotype in the previous experiment.
269 We aerosol infected *Ccr2-/-* mice with a mixed 1:1 bacterial suspension of WT *M. kansasii* and *M.*
270 *kansasii*::*Rv3377-78c* (Fig. 7b). Interestingly, although WT *M. kansasii* exhibited a slight increase
271 in numbers over time, *M. kansasii*::*Rv3377-78c* steadily decreased within the same period. A
272 statistically significant decrease in the *M. kansasii*::*Rv3377-78c* to WT *M. kansasii* ratio over time
273 was noted, with a steady, non-stabilizing decrease in the proportion of *M. kansasii*::*Rv3377-78c*
274 in the bacterial population (Fig. 7b). Thus, *M. kansasii*::*Rv3377-78c* was clearly outcompeted by
275 WT *M. kansasii* in both of these *in vivo* infection models.
276
277 **DISCUSSION**
278 Our results indicate the feasibility of using *M. kansasii* to study the pathoevolution of *M.*
279 *tuberculosis*. The less virulent non-tuberculous mycobacterium (NTM) species is a suitable
280 surrogate for the expression of *M. tuberculosis*-specific products, such as 1-TbAd, and can readily
281 be used *in vitro*, and for *ex vivo* and *in vivo* experimental infection models. We showed that 1-
282 TbAd led to an improved survival during the first 24 hours of infection when tested *in vivo*, and
283 *ex vivo* in alveolar macrophages, but the isolated addition of 1-TbAd to *M. kansasii* resulted in
284 impaired persistence in different murine infection models.
285
286 In the current study, we demonstrated that *M. kansasii::Rv3377-78c* produced lipid
287 species distinct from those seen in *M. kansasii*::EV. Our prior and current data indicated that
288 transfer of TbAd biosynthesis genes to *M. kansasii* does not promote growth at neutral pH, but

289 confers increased growth in 7H9 media in the more acidic pH range (5.0-5.4) (22). When added
290 as a pure compound or produced by *M. tuberculosis*, 1-TbAd detectably raises the pH and swells
291 lysosomes in human macrophages (18, 22). In broad terms, the mechanisms by which the effects
292 of 1-TbAd are mediated could occur through direct chemical results of lysosomotropism, or
293 through signalling.
294
295 1-TbAd could act as an amphipathic weak base that penetrates membranes as an
296 uncharged conjugate base to selectively accumulate in acidic phagolysosomes where proton
297 capture raises pH and confers a positive charge, trapping the compound and leading to lysosomal
298 swelling. We did not see clear *Rv3377-Rv3378c*-dependent alkalization of 7H9 broth which might
299 be explained by compartmentalization: whereas intracellular bacteria are bound in a small
300 phagosomal compartment of 10^{-15} L, growth in 7H9 media provides a much larger compartment
301 for 1-TbAd to disperse in if it is physically shed from the bacterium. By a rough estimate, 10^{10}
302 bacteria-worth of 1-TbAd would be required to change the pH of 1 ml of 7H9 from 5.2 to 5.3,
303 about 10,000 times the concentration of bacteria we inoculate (see supplementary data
304 calculation). This result suggested that 1-TbAd production provides a pH-dependent growth
305 advantage intrinsic to the bacterium, separate from but not exclusive to lysosomal perturbation.
306
307 In phagocyte-free systems, we experimentally tested the hypothesis that the pH-
308 dependent growth advantage of *M. kansasii* producing 1-TbAd might involve direct contact of
309 the molecules with bacteria. Overall we found that direct exposure to externally added,
310 protonated 1-TbAd at low and high concentrations did not promote growth as might be expected

311 of a signaling molecule. Increased growth was selectively observed at low pH (5.1-5.4) when 1-
312 TbAd was generated through gene transfer and the action of enzymes in the bacterium. While
313 not fully understood, these divergent outcomes whereby the compartment of origin controls the
314 protective effect can be explained by the lysosomotropy model. Cytosolic 1-TbAd would be
315 expected to shed its proton during membrane passage into the periplasm. The lack of pH control
316 in the cytosol of *M. kansasii::Rv3377-78c* cultured in acidic media suggests that 1-TbAd does not
317 act as a shield against proton flow into *M. kansasii* cytosol, which is the expected outcome if
318 membrane penetration is required for the protective effect. These outcomes indicate that the
319 consistently observed survival advantage could derive from 1-TbAd passage from the cytosolic
320 membrane into the periplasm, mycolate membrane or surface of *M. kansasii*. 1-TbAd may act
321 on the bacterial population itself by targeting or protecting specific molecules during exposure
322 to low pH, stopping damage from occurring.
323
324 It is noteworthy that genetic and chemical complementation provide different
325 information about mycobacterial virulence factors, which in this case might result from the
326 differential compartmentalization of the molecules. This result also argues that 1-TbAd must
327 exert its protective effect at a specific location within the bacterial cell or cell wall. Exogenous 1-
328 TbAd may simply not reach this specific location, or not reach the location in an uncharged
329 conjugate base state. Together with our genetic complementation data, it is clear that *Rv3377c-*
330 *Rv3378c*-dependent metabolites including 1-TbAd do not have a direct growth-promoting effect.
331 Our data also demonstrate that *Rv3377c-Rv3378c*-dependent metabolites protect against acid

332 stress *in vitro*, using mechanisms that are independent of macrophage function, including
333 lysosomes or activating receptors.
334
335 Another key finding is that the complemented strain fared better than *M. kansasii*::EV in
336 the initial stages of *in vivo* infection. We subsequently showed that *M. kansasii*::*Rv3377-78c* was
337 more fit to thrive inside alveolar macrophages, but not bone marrow-derived macrophages
338 within that same timeframe, demonstrating that the production of 1-TbAd can subvert the first
339 lines of host defense encountered by the pathogen. Reasons for the observed increased survival
340 in alveolar macrophages might include 1-TbAd inducing acid tolerance that enables the bacteria
341 to survive the conditions inside the phagolysosome.
342
343 WT *M. kansasii* eventually outcompeted *M. kansasii*::*Rv3377-78c* in low- and high-dose
344 mixed infection settings in both WT and *Ccr2*-/- mice. Therefore, although expression of *Rv3377c-*
345 *Rv33778c* conferred a survival benefit to *M. kansasii* in specific *in vitro* and short-term infection
346 contexts, it appears there is a drawback to 1-TbAd expression in the non-adapted mycobacterium
347 for persisting in the murine host. We hypothesize that the burden of constitutive production of
348 1-TbAd, which sequesters adenosine molecules, may prevent energy storage in the form of ATP
349 and have a negative impact on long-term *in vivo* survival for *M. kansasii*. Another consideration
350 is the extent to which mycobacterial killing is dependent on acid-mediated mechanisms. The
351 intrinsic antacid properties of 1-TbAd, its tropism for acid compartments, its marked remodeling
352 of lysosomes and the pH-dependent basis of growth promotion in culture media all point at a
353 selective role in protection against acid-mediated killing. Therefore, the varied outcomes in the

354 models examined herein might depend on the extent to which they test acid-dependent killing.
355 One question that remains unanswered is whether there is a single, predominant mechanism of
356 action for which 1-TbAd production is mainly conserved in *M. tuberculosis*, or multiple important
357 functions.
358
359 Phenotypes observed after pathogen-specific genetic complementation into non-
360 pathogenic species provide different information than the more commonly observed loss-of-
361 function phenotypes observed after deleting genes from pathogens. The latter requires breaking
362 one link in a causal chain and might have rippling downstream effects, if it is not the final
363 component of a response cascade. Gain of function is a rare phenomenon that occurs only when
364 the components of a larger pathogen-specific system are fully recapitulated in the non-pathogen
365 and then tested under conditions in which this system is essential. In this regard, that
366 biosynthetic genes for 1-TbAd can promote early stage growth in alveolar macrophages was
367 unexpected, so these data now point to a new direction for mechanistic studies of these genes
368 in *M. tuberculosis*.
369
370 To date, the established virulence factors of *M. tuberculosis* are largely conserved among
371 the NTM, with the exception of 1-TbAd, Tuberculosis Necrotizing Toxin (32) and the MoaA1-4
372 operon (33). Our data indicate that 1-TbAd alone does not confer a long-term *in vivo* benefit
373 consistent with *in vitro* and *in vivo* phenotypic differences between *M. tuberculosis* and *M.*
374 *kansasii*. Therefore, events of acquisition of other *M. tuberculosis*-specific and loss of *M. kansasii*-
375 specific effectors are likely required to recreate an *M. tuberculosis*-like *M. kansasii* mutant strain,

376 or alternatively the difference is due to the compounding of multiple subtle effects that
377 complement one another. The possibility that mycobacterial virulence factors manifest their
378 phenotype in a cell-dependent fashion is consistent with the known transcellular lifestyle of *M.*
379 *tuberculosis* and suggests that different host-cell types should be used to detect undiscovered
380 virulence determinants.
381
382 Viewed in this light, using genetically complemented NTM is therefore useful to single out
383 the effects of specific elements that contributed to *M. tuberculosis* host adaptation without
384 producing a clearly hypervirulent NTM. The 1-TbAd family of molecules represents a newly
385 discovered pathogen-specific collection of compounds that has no clear chemical analog in other
386 bacterial systems, and their exact mechanisms of action remain elusive. We can conclude from
387 our study that *Rv3377c-Rv3378c* transfer acts in a eukaryotic cell-free system by a localized
388 chemical mechanism that involves pH, and that such changes can be determinative of outcomes
389 in alveolar macrophages at expectedly early time points post-infection. As such, these molecules
390 may aid in the establishment of infection within the lower respiratory tract.
391
392 **MATERIALS AND METHODS**
393 **Bacterial strains and culture conditions**
394 *M. kansasii* ATCC 12478 and *M. tuberculosis* H37Rv were grown in Middlebrook 7H9 broth (BD
395 Difco, MD, USA) as previously described (3). To test the ability of *M. kansasii*::*Rv3377-78c* to
396 produce yellow pigment, fully-formed colonies were additionally exposed to white light and
397 incubated at room temperature for 7 days. Where indicated and to ensure single-cell

398 suspensions, liquid bacterial cultures were de-clumped by slowly passaging through 5x 22G, 5x
399 25-G and 3x 26-G needles followed by low-speed centrifugation at 50 g for 5 minutes with
400 passage through a 5-µm filter. To generate *M. kansasii*::*Rv3377-78c*, a 2.4-kb PCR fragment
401 spanning *Rv3377c-Rv3378c* was generated using primers BamHI-*Rv3377c-Rv3378c*-F and HindIII-
402 *Rv3377c-Rv3378c*-R (Sup. Table 1) using high-fidelity Phusion DNA polymerase (New England
403 Biolabs). The fragment was subsequently digested with BamHI and HindIII (all restriction enzymes
404 from New England Biolabs) and cloned into the episomal plasmid pMV261 with the constitutive
405 mycobacterial *hsp60* promoter and a selective apramycin resistance marker. The *hsp60-Rv3377c-*
406 *Rv3378c* fragment was shuttled into the integrative vector pMV306 containing a hygromycin
407 resistance cassette using XbaI and HindIII. All ligations were done using T4 DNA ligase
408 (Fermentas). The resulting plasmid pMV306::*Hsp60-Rv3377c-Rv3378c* was verified by Sanger
409 sequencing (Genome Québec) to ensure the absence of frameshift or point mutations during the
410 cloning process. An unaltered version of pMV306 with a hygromycin resistance cassette was used
411 to create the empty vector control strain *M. kansasii*::EV. Following electroporation, *M.*
412 *kansasii*::EV and *M. kansasii*::*Rv3377-78c* were grown in the presence of 100 µg/mL hygromycin
413 (Wisent).
414
415 **Detection of cell filtrate adenosine-linked lipids**
416 *M. kansasii*::EV, *M. kansasii*::*Rv3377-78c* and *M. tuberculosis* were grown to mid-log phase and
417 subsequently incubated with 0.25 µCi/mL radiolabeled [8-^{14}C]adenosine (American Radiolabeled
418 Chemicals) for 14 days. Polar lipid fractions were extracted using $CHCl_3$:CH_3OH:0.3%NaCl
419 (v/v/v)(22).)(34). Extracted lipids were spotted on a TLC Silica Gel 60 (Millipore Sigma) with

420 $CHCl_3$:CH_3OH:H_2O 10:5:1 (v/v/v) used as the mobile phase solvent. The radiolabeled signature
421 was developed using Storm 840 PhosphorImager (GE Healthcare) to visualize adenosine-linked
422 lipids in each lane. [8-^{14}C]adenosine 1:100 was used as a no-lipid staining control. The plate was
423 stained with 5% phosphomolybdic acid reagent (PMA) (Sigma) and heated briefly using an
424 industrial blow-dryer to visualize the total amounts of lipids loaded in each lane.
425
426 **HPLC-MS analysis of lipids from cells and supernatant**
427 *M. kansasii::Rv3377-78c*, *M. kansasii::*Empty vector (EV) and *M. kansasii* parent strain were
428 grown in 30 ml of 7H9 media supplemented with albumin-dextrose-saline (5% Bovine Serum
429 Albumin Fraction V, 2% anhydrous dextrose and 0.87% sodium chloride) to late log-phase.
430 Bacterial cell pellet and supernatant were separated by centrifugation at 5000 rpm for 5 minutes.
431 The cell pellet was resuspended in 4 ml of PBS at pH 7.4 and distributed equally into four 2 ml
432 screw-cap tubes. The cells were pelleted by centrifugation and further resuspended in 1 ml PBS
433 at pH titrated to 7.4, 6.4, 5.5 and 4.5 with hydrochloric acid and incubated for 2 hours at 37°C. At
434 the end of 2 hours the cell pellet and the PBS supernatant were collected for lipid extraction.
435 Added 10 volumes (3 ml) of Chloroform/methanol (C/M) at the ratio of 1:2 and extracted for 1
436 hour at room temperature. A second extraction under similar conditions was performed with 3
437 ml of C/M at the ratio of 1:1. The extracted fractions were pooled and dried under a stream of
438 nitrogen gas. Lipids from the 1 ml PBS supernatant was extracted using acidified ethyl acetate by
439 adding 3 µl of 6N HCl and 1.4 ml of ethyl acetate and mixing for 30 minutes in an Orbitron shaker.
440 The mixture was centrifuged at 2000 rpm for 15 minutes to collect the upper organic phase and
441 dried on to glass under a stream of nitrogen gas at room temperature, and total lipids were

442 weighed using analytical balance. HPLC-MS separations were performed as described (17) using
443 equal amount of lipid samples from different experimental conditions as determined by weight
444 on a Mettler balance.
445
446 **Congo Red uptake assay**
447 Bacterial cultures were grown on Congo Red-containing 7H10 plates for 14 days, scraped into a
448 15-ml conical tube, washed with water until the supernatant became clear and incubated with 2
449 ml DMSO for 2 hours (24, 35). Congo Red was measured in the resultant supernatant at A488.
450 The values were normalized to the dry weight of the pellet to define the Congo Red binding index.
451
452 **Extracellular pH measurement**
453 For all pH experiments, liquid media was prepared as usual and the pH was equilibrated to 4.0,
454 4.9, 5.0, 5.1, 5.2, 5.4, 6.0, 6.7 and 7.2 using 2 M HCl or NaOH. OD_{600} was adjusted to 0.34 and 222
455 µl of mid-log phase de-clumped bacteria were added to 15 ml of freshly prepared, pH-adjusted
456 7H9 in 150-ml roller bottles (final OD_{600} of 0.005). Triplicate cultures were made per condition
457 (strain and pH) and incubated at 37°C, rolling in the dark. OD_{600} was measured every 2-3 days
458 using 2 x 200 µl of culture (technical duplicates) and a Tecan Infinite M200 Pro plate reader. At
459 days 8 and 17, 1 ml was removed from each culture for centrifugation and recovery of
460 supernatant, which was stored at 4°C until extracellular pH was read using micro pH combination
461 electrode (AgCl) (Sigma Aldrich), and Orion Star A111 meter (Thermo Scientific).
462
463

464

465 **Synthetic TbAds and chemical complementation**

466 Synthetic 1-TbAd and N^6-TbAd were produced as described previously (36). Bacterial cultures
467 were grown to mid-log phase and de-clumped as described above, then inoculated into 96-well
468 plates in 200 µl pH-adjusted 7H9 containing 1-TbAd, N^6-TbAd or vehicle (DMSO) control as
469 indicated. Plates were incubated at 37°C in the dark and OD_{600} was measured every one to three
470 days with a Tecan Infinite M200 Pro plate reader.

471

472 **Intracellular pH measurement**

473 Bacterial cultures were grown to mid-log phase and de-clumped as previously described. $5x10^8$
474 CFU were pelleted, the supernatant completely removed, and the cells resuspended in 0.3 ml
475 PBS containing 100 µM Carboxyfluorescein diacetate succinimidyl ester (CFDA-SE) (CellTrace™
476 CFSE, ThermoFisher) for 20 minutes at 37°C, shaking at 150 RPM in the dark. Bacteria were next
477 diluted with 10 ml of 7H9 and incubated for 4 hours at 37°C, rolling in the dark. A portion of
478 bacteria was taken during this incubation for lysis in normal saline (0.9% NaCl) by beating with
479 silica beads (MP Biomedicals, FastPrep-24) to extract free protein-CFSE conjugate to generate a
480 fluorescence-to-pH standard curve. After 4 hours, bacteria were washed and resuspended in
481 normal saline to an OD_{600} of 0.4. 20 µl of bacteria in saline were sub-cultured into 180 µl of freshly
482 prepared, pH-adjusted 7H9 in 96-well plates (opaque-black for fluorescence (ThermoScientific
483 Nunclon Delta Surface), translucent-colourless for absorbance (Falcon). Lysed bacteria were
484 plated similarly for the pH standard curve. Immediately, plates were placed in plate readers
485 (Tecan Infinite M200 Pro) at 37°C, shaking and measuring fluorescence or OD_{600} every 30

486 minutes. 528-nm fluorescence was measured from 490-nm excitation (pH-sensitive), and 520-
487 nm fluorescence was measured from 450-nm excitation (pH-insensitive). To calculate pH, 7H9
488 background was subtracted for all data first (pH did not alter 7H9 fluorescence). Next, a standard
489 curve of 490-excitation/450-excitation in relation to 7H9 pH was created from the CFSE-
490 containing cell lysate. The 490/450 ratios calculated from the culture wells were applied to the
491 standard curve to determine intracellular pH.
492
493 **Murine pulmonary infection**
494 C57Bl/6 and *Ccr2-/-* mice (Jackson Laboratories) of approximately 6 to 20 weeks of age were used
495 for experiments. All protocols were approved by independent ethics oversight at the RI-MUHC
496 and followed the guidelines of the Canadian Council on Animal Care (CCAC). C57Bl/6 mice were
497 infected through aerosolization (ONARES, NJ, USA) of bacterial cultures at OD_{600} 0.4 for 15
498 minutes as previously described (3). Alternatively, C57Bl/6 mice were infected via trans-laryngeal
499 intubation using 50 µl of a high-dose mixed bacterial suspension containing both wild-type (WT)
500 *M. kansasii* and *M. kansasii*::*Rv3377-78c* at OD_{600} 0.2. C57Bl/6 *Ccr2-/-* (C-C motif chemokine
501 receptor 2 knockout) mice were infected through aerosolization of a low-dose mixed suspension
502 at OD_{600} 1.0. Mouse lungs were harvested at 4 or 24 hours (early time-points to measure short-
503 term bacterial establishment) and 14, 21, 28, 42 or 56 days post infection (later time-points to
504 measure long-term bacterial persistence) into 1ml 7H9 and homogenized using an Omni Tissue
505 Homogenizer TH (Omni International) at high speed for 45 seconds. Serial dilutions made in 7H9
506 liquid media from lung homogenates were plated on 7H10 plates containing PANTA ± 50 µg/ml

507 hygromycin. Colony-forming units (CFU) were counted 2 weeks post-plating to determine
508 bacterial burden.
509
510 **Murine macrophage isolation**
511 Bone marrow was isolated from C57Bl/6 murine tibiae and femora. Bone marrow-derived
512 macrophage (BMDMs) were differentiated with recombinant M-CSF (100 U/ml) (Peprotech) for
513 a period of 7 days as previously described (37), after which they were lifted using 4 ml CellStripper
514 Solution (Corning) and seeded into the appropriate tissue-culture plates. For alveolar
515 macrophage (AM) isolation, the respiratory tract including the trachea and lungs was isolated
516 and repeatedly perfused with cold sterile phosphate-buffered saline (PBS) to collect the cells
517 through bronchoalveolar lavage (BAL). AMs were enriched through adherence purification to
518 tissue culture-treated 96-well plates over 24 hours, at which point other cells were washed away.
519 All mammalian cells were cultured in RPMI 1640 media supplemented with non-essential amino
520 acids, 10 mM HEPES, 10% FBS ± Penicillin/Streptomycin (Wisent).
521
522 **Macrophage infection**
523 Macrophages were seeded into 96-well plates (100,000 cells/200 µl complete RPMI media
524 without antibiotics). Bacterial cultures were grown to OD_{600} 0.2-0.5, clumps were removed to
525 ensure single-cell suspensions and adjusted in complete RPMI media (without antibiotics) to an
526 OD_{600} 0.01. Macrophages were infected by replacing the media with fresh media containing
527 bacterial suspension. After 4 hours of infection, the wells were gently washed three times with
528 PBS to remove extracellular bacteria and fresh complete RPMI media (without antibiotics) was

529 added to each well. At indicated time points, the plates were spun down at 2,000 g for 5 minutes.
530 Each well was subjected to PBS containing 1% Triton X-100 for 10 minutes at room temperature
531 to induce macrophage lysis. Following serial dilution and plating, CFUs were counted on 7H10
532 plates 2 weeks post-plating to determine bacterial burden.
533

534 **Statistical analysis**

535 All calculations and statistical analyses were performed using Microsoft Excel or GraphPad Prism.
536 Calculations included (1) the ratio of individual 24-hr CFU values/mean 4-hr CFU for murine lung
537 and macrophage infection assays to determine bacterial proliferation [datapoint = (24-hr
538 CFU)/(mean 4-hr CFU)] and (2) the proportion of *MKAN::Rv33778c /* total (values paired from
539 individual mice) in competition assays to determine comparative fitness of WT *M. kansasii* vs. *M.*
540 *kansasii*::*Rv3377-78c* [datapoint = (CFU on 7H10-Hygromycin)/(CFU on 7H10)].
541

542 **Acknowledgements**

543 We would like to thank Dr. Maziar Divangahi and Laura Mendonça for transferring their
544 knowledge on alveolar macrophages and for providing *Ccr2*-/- mice. We would also like to thank
545 Dr. David Young for assistance with chromatography and figure preparation.
546 This project was funded through the support of an operating CIHR grant FND-148362.
547

548 **References**

549 1. Peirs P, Lefevre P, Boarbi S, Wang XM, Denis O, Braibant M, Pethe K, Locht C, Huygen K,
550 Content J. 2005. Mycobacterium tuberculosis with disruption in genes encoding the

551 phosphate binding proteins PstS1 and PstS2 is deficient in phosphate uptake and
552 demonstrates reduced in vivo virulence. Infect Immun 73:1898-902.
553 2. Dunphy KY, Senaratne RH, Masuzawa M, Kendall LV, Riley LW. 2010. Attenuation of
554 Mycobacterium tuberculosis functionally disrupted in a fatty acyl-coenzyme A synthetase
555 gene fadD5. J Infect Dis 201:1232-9.
556 3. Wang J, McIntosh F, Radomski N, Dewar K, Simeone R, Enninga J, Brosch R, Rocha EP,
557 Veyrier FJ, Behr MA. 2015. Insights on the emergence of Mycobacterium tuberculosis
558 from the analysis of Mycobacterium kansasii. Genome Biol Evol 7:856-70.
559 4. Bloch KC, Zwerling L, Pletcher MJ, Hahn JA, Gerberding JL, Ostroff SM, Vugia DJ, Reingold
560 AL. 1998. Incidence and clinical implications of isolation of Mycobacterium kansasii:
561 results of a 5-year, population-based study. Ann Intern Med 129:698-704.
562 5. Johnson MM, Odell JA. 2014. Nontuberculous mycobacterial pulmonary infections. J
563 Thorac Dis 6:210-20.
564 6. Sheu LC, Tran TM, Jarlsberg LG, Marras TK, Daley CL, Nahid P. 2015. Non-tuberculous
565 mycobacterial infections at San Francisco General Hospital. Clin Respir J 9:436-42.
566 7. Ricketts WM, O'Shaughnessy TC, van Ingen J. 2014. Human-to-human transmission of
567 Mycobacterium kansasii or victims of a shared source? Eur Respir J 44:1085-7.
568 8. Griffith DE, Aksamit T, Brown-Elliott BA, Catanzaro A, Daley C, Gordin F, Holland SM,
569 Horsburgh R, Huitt G, Iademarco MF, Iseman M, Olivier K, Ruoss S, von Reyn CF, Wallace
570 RJ, Jr., Winthrop K, Subcommittee ATSMD, American Thoracic S, Infectious Disease
571 Society of A. 2007. An official ATS/IDSA statement: diagnosis, treatment, and prevention
572 of nontuberculous mycobacterial diseases. Am J Respir Crit Care Med 175:367-416.

573 9. Fortune SM, Jaeger A, Sarracino DA, Chase MR, Sassetti CM, Sherman DR, Bloom BR,
574 Rubin EJ. 2005. Mutually dependent secretion of proteins required for mycobacterial
575 virulence. Proc Natl Acad Sci U S A 102:10676-81.
576 10. Boon C, Dick T. 2002. Mycobacterium bovis BCG response regulator essential for hypoxic
577 dormancy. J Bacteriol 184:6760-7.
578 11. Walters SB, Dubnau E, Kolesnikova I, Laval F, Daffe M, Smith I. 2006. The Mycobacterium
579 tuberculosis PhoPR two-component system regulates genes essential for virulence and
580 complex lipid biosynthesis. Mol Microbiol 60:312-30.
581 12. Salah IB, Ghigo E, Drancourt M. 2009. Free-living amoebae, a training field for
582 macrophage resistance of mycobacteria. Clin Microbiol Infect 15:894-905.
583 13. Veyrier F, Pletzer D, Turenne C, Behr MA. 2009. Phylogenetic detection of horizontal gene
584 transfer during the step-wise genesis of Mycobacterium tuberculosis. BMC Evol Biol
585 9:196.
586 14. Becq J, Gutierrez MC, Rosas-Magallanes V, Rauzier J, Gicquel B, Neyrolles O, Deschavanne
587 P. 2007. Contribution of horizontally acquired genomic islands to the evolution of the
588 tubercle bacilli. Mol Biol Evol 24:1861-71.
589 15. Boritsch EC, Khanna V, Pawlik A, HonorÈ N, Navas VH, Ma L, Bouchier C, Seemann T,
590 Supply P, Stinear TP, Brosch R. 2016. Key experimental evidence of chromosomal DNA
591 transfer among selected tuberculosis-causing mycobacteria. Proceedings of the National
592 Academy of Sciences of the United States of America 113:9876-81.

593 16. Sapriel G, Brosch R. 2019. Shared pathogenomic patterns characterize a new phylotype,
594 revealing transition towards host-adaptation long before speciation of Mycobacterium
595 tuberculosis. Genome Biol Evol doi:10.1093/gbe/evz162.
596 17. Layre E, Lee HJ, Young DC, Martinot AJ, Buter J, Minnaard AJ, Annand JW, Fortune SM,
597 Snider BB, Matsunaga I, Rubin EJ, Alber T, Moody DB. 2014. Molecular profiling of
598 Mycobacterium tuberculosis identifies tuberculosinyl nucleoside products of the
599 virulence-associated enzyme Rv3378c. Proc Natl Acad Sci U S A 111:2978-83.
600 18. Young DC, Layre E, Pan SJ, Tapley A, Adamson J, Seshadri C, Wu Z, Buter J, Minnaard AJ,
601 Coscolla M, Gagneux S, Copin R, Ernst JD, Bishai WR, Snider BB, Moody DB. 2015. In vivo
602 biosynthesis of terpene nucleosides provides unique chemical markers of Mycobacterium
603 tuberculosis infection. Chem Biol 22:516-526.
604 19. Mann FM, Xu M, Chen X, Fulton DB, Russell DG, Peters RJ. 2009. Edaxadiene: a new
605 bioactive diterpene from Mycobacterium tuberculosis. J Am Chem Soc 131:17526-7.
606 20. Lau SK, Lam CW, Curreem SO, Lee KC, Lau CC, Chow WN, Ngan AH, To KK, Chan JF, Hung
607 IF, Yam WC, Yuen KY, Woo PC. 2015. Identification of specific metabolites in culture
608 supernatant of Mycobacterium tuberculosis using metabolomics: exploration of potential
609 biomarkers. Emerg Microbes Infect 4:e6.
610 21. David HL. 1974. Carotenoid pigments of Mycobacterium kansasii. Appl Microbiol 28:696-
611 9.
612 22. Buter J, Cheng TY, Ghanem M, Grootemaat AE, Raman S, Feng X, Plantijn AR, Ennis T,
613 Wang J, Cotton RN, Layre E, Ramnarine AK, Mayfield JA, Young DC, Jezek Martinot A,
614 Siddiqi N, Wakabayashi S, Botella H, Calderon R, Murray M, Ehrt S, Snider BB, Reed MB,

615 Oldfield E, Tan S, Rubin EJ, Behr MA, van der Wel NN, Minnaard AJ, Moody DB. 2019.
616 Mycobacterium tuberculosis releases an antacid that remodels phagosomes. Nat Chem
617 Biol 15:889-899.
618 23. de Duve C, Trouet A, Campeneere DD, Baurian R. 1978. Liposomes as lysosomotropic
619 carriers. Ann N Y Acad Sci 308:226-34.
620 24. Jankute M, Nataraj V, Lee OY, Wu HHT, Ridell M, Garton NJ, Barer MR, Minnikin DE, Bhatt
621 A, Besra GS. 2017. The role of hydrophobicity in tuberculosis evolution and pathogenicity.
622 Sci Rep 7:1315.
623 25. Portaels F, Pattyn SR. 1982. Growth of mycobacteria in relation to the pH of the medium.
624 Ann Microbiol (Paris) 133:213-21.
625 26. Vandal OH, Nathan CF, Ehrt S. 2009. Acid resistance in Mycobacterium tuberculosis. J
626 Bacteriol 191:4714-21.
627 27. Pethe K, Swenson DL, Alonso S, Anderson J, Wang C, Russell DG. 2004. Isolation of
628 Mycobacterium tuberculosis mutants defective in the arrest of phagosome maturation.
629 Proc Natl Acad Sci U S A 101:13642-7.
630 28. Stewart GR, Patel J, Robertson BD, Rae A, Young DB. 2005. Mycobacterial mutants with
631 defective control of phagosomal acidification. PLoS Pathog 1:269-78.
632 29. Johnson JD, Hand WL, King NL, Hughes CG. 1975. Activation of alveolar macrophages after
633 lower respiratory tract infection. J Immunol 115:80-4.
634 30. Guilbault C, Martin P, Houle D, Boghdady ML, Guiot MC, Marion D, Radzioch D. 2005.
635 Cystic fibrosis lung disease following infection with Pseudomonas aeruginosa in Cftr

636 knockout mice using novel non-invasive direct pulmonary infection technique. Laboratory
637 Animals 39:336-352.
638 31. Peters W, Scott HM, Chambers HF, Flynn JL, Charo IF, Ernst JD. 2001. Chemokine receptor
639 2 serves an early and essential role in resistance to Mycobacterium tuberculosis. Proc Natl
640 Acad Sci U S A 98:7958-63.
641 32. Pajuelo D, Gonzalez-Juarbe N, Tak U, Sun J, Orihuela CJ, Niederweis M. 2018. NAD(+)
642 Depletion Triggers Macrophage Necroptosis, a Cell Death Pathway Exploited by
643 Mycobacterium tuberculosis. Cell Rep 24:429-440.
644 33. Levillain F, Poquet Y, Mallet L, Mazeres S, Marceau M, Brosch R, Bange FC, Supply P,
645 Magalon A, Neyrolles O. 2017. Horizontal acquisition of a hypoxia-responsive
646 molybdenum cofactor biosynthesis pathway contributed to Mycobacterium tuberculosis
647 pathoadaptation. PLoS Pathog 13:e1006752.
648 34. Slayden RA, Barry CE, 3rd. 2001. Analysis of the Lipids of Mycobacterium tuberculosis.
649 Methods Mol Med 54:229-45.
650 35. Cangelosi GA, Palermo CO, Laurent JP, Hamlin AM, Brabant WH. 1999. Colony
651 morphotypes on Congo red agar segregate along species and drug susceptibility lines in
652 the Mycobacterium avium-intracellulare complex. Microbiology 145 (Pt 6):1317-24.
653 36. Buter J, Heijnen D, Wan IC, Bickelhaupt FM, Young DC, Otten E, Moody DB, Minnaard AJ.
654 2016. Stereoselective Synthesis of 1-Tuberculosinyl Adenosine; a Virulence Factor of
655 Mycobacterium tuberculosis. J Org Chem 81:6686-96.
656 37. Zhang X, Goncalves R, Mosser DM. 2008. The isolation and characterization of murine
657 macrophages. Curr Protoc Immunol Chapter 14:Unit 14 1.

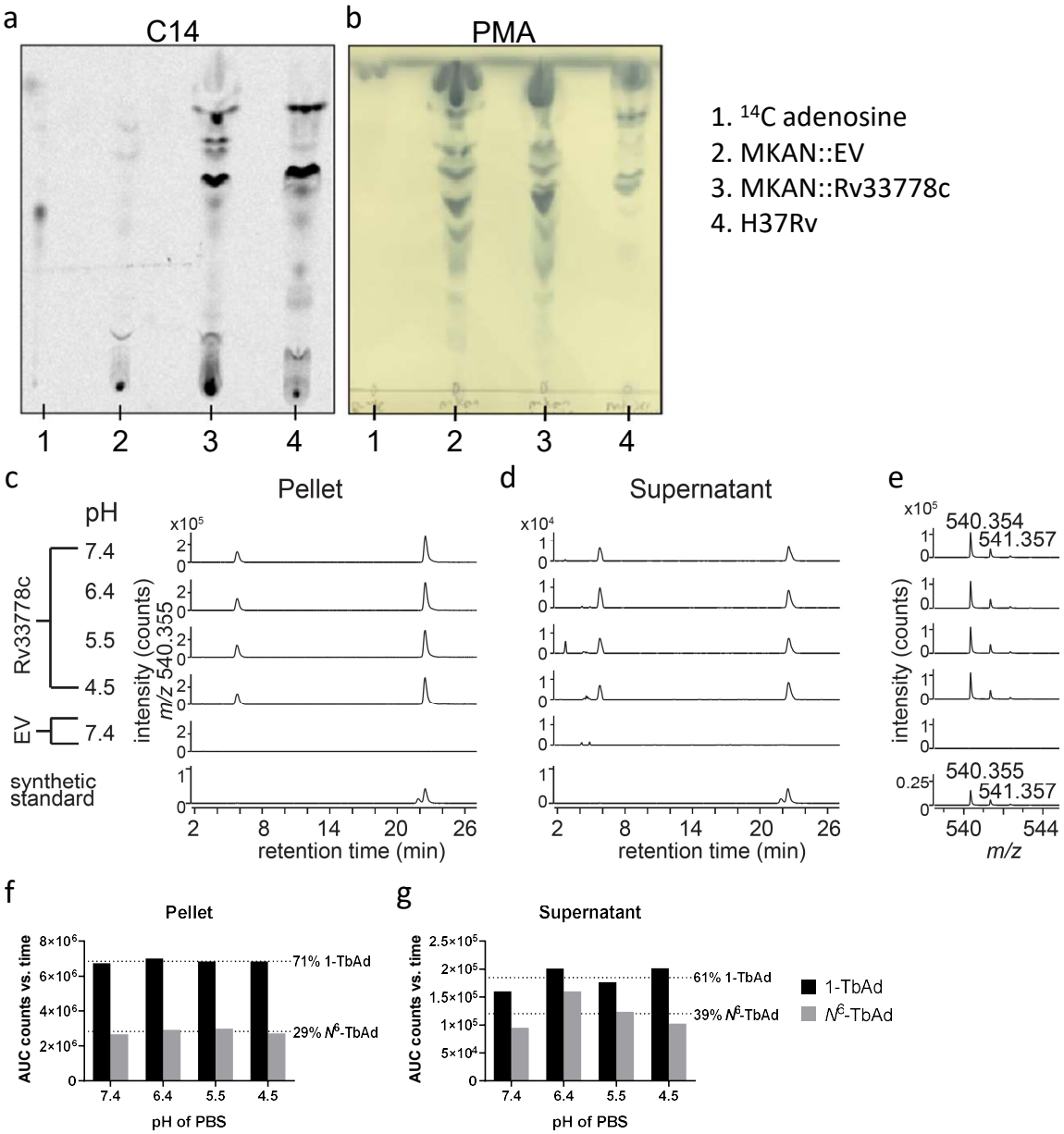

Figure 1 – *M. kansasii::*Rv3377-78c produces adenosine-linked lipids 1-TbAd and N6-TbAd. (a) Detection of adenosine-linked lipids extracted from *M. kansasii::*EV (MKAN::EV), *M. kansasii::Rv3377-78c* (MKAN::Rv33778c) and *M. tuberculosis* (H37Rv) through radiolabelling and separation using normal-phase silica thin-layer chromatography. (b) Visualization of migration pattern of total lipids from each sample after staining with 5% phosphomolybdic acid reagent. (c-e) Lipids from *M. kansasii* derived from cell pellets or culture supernatant incubated for two hours at the indicated pH, neutralized and then extracted with organic solvent. Product was analyzed in comparison with a synthetic standard for 1-TbAd. (e) The mass spectrum of lipids extracted from 21-22 min for *M. kansasii* show a m/z value that matches with the measured and expected mass of a 1-TbAd standard (21) (f-g) Total extracted lipids expressed as area under curve from counts versus retention time of the extracted ion chromatogram. 1.0uM of synthetic 1-TbAd was used as the standard.

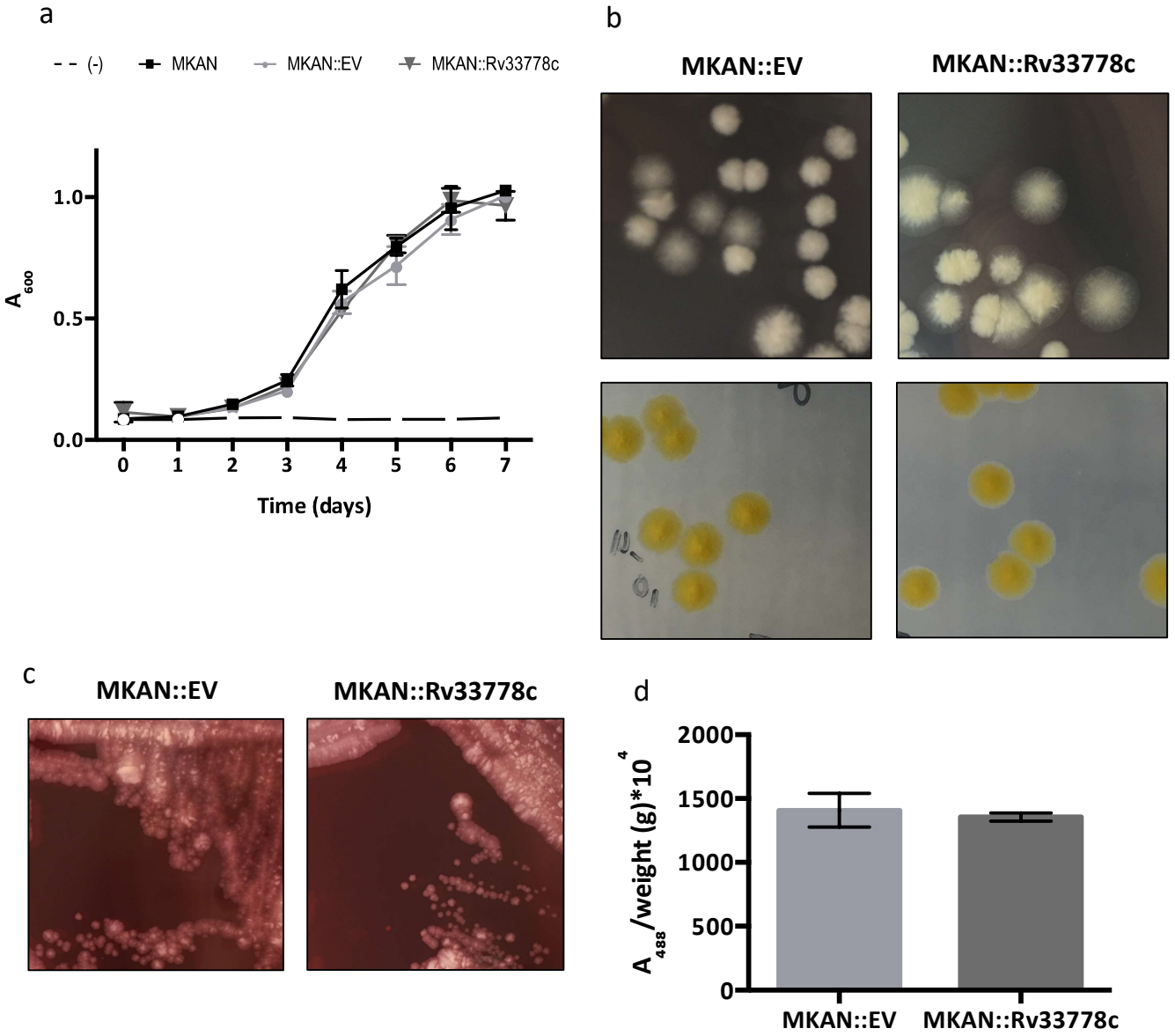

Figure 2 – 1-TbAd production does not influence the *in vitro* growth characteristics and behaviours of *M. kansasii*. (a) Comparative OD_{600} growth kinetics of wild-type *M. kansasii* (MKAN), *M. kansasii*::EV *(*MKAN::EV) and *M. kansasii*::*Rv3377-78c* (MKAN::Rv33778c) at 37ºC in 7H9 broth. The data are presented as the mean of technical triplicates ± SD. The data are representative of three independent experiments. (b) Colony morphology in 2 different incubation settings of *M. kansasii*::EV (MKAN::EV) and *M. kansasii*::*Rv3377-78c* (MKAN::Rv33778c) on 7H10 plates. (c) Colony morphology of *M. kansasii*::EV (MKAN::EV) and *M. kansasii*::*Rv3377-78c* (MKAN::Rv33778c) on 7H10 plates supplemented with Congo Red. (d) Quantitative analysis of Congo Red dye retention by *M. kansasii:*:EV (MKAN::EV) and *M. kansasii*::*Rv3377-78c* (MKAN::Rv33778c). DMSO extraction was followed by absorbance at 488nm divided by the weight of the dry culture pellet after washing (in grams). The data are plotted as the mean of technical triplicates ± SD. The data are representative of two independent experiments.

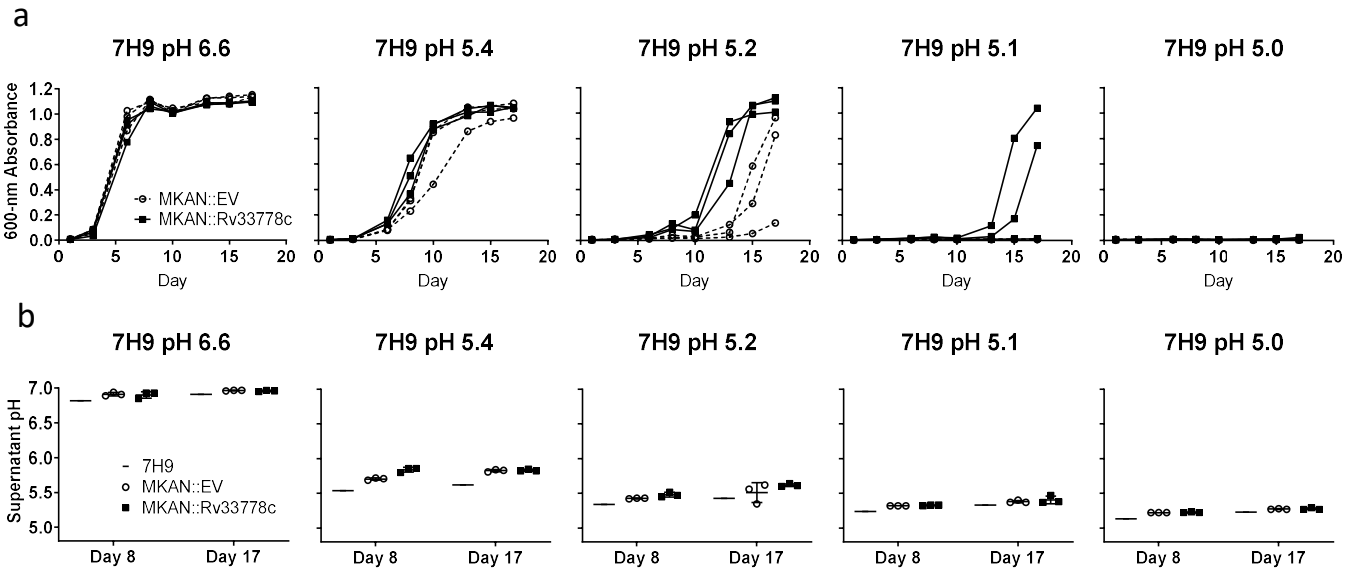

Figure 3 – 1-TbAd production enhances growth at low pH where growth is associated with culture medium alkalization. *M. kansasii::*EV (MKAN::EV) and *M. kansasii*::*Rv3377-78c* (MKAN::Rv33778c) cultures were inoculated at equal OD_{600} into fresh pH-adjusted 7H9 (using HCl titration) and incubated at 37ºC in a rolling incubator over 17 days. The starting pH of the cultures is indicated above each graph. (a) OD_{600} was monitored every 2-3 days. The data are plotted separately for each of three independently growing cultures per strain. The data are representative of 5 independent experiments. (b) The pH of the supernatant was measured at days 8 and 17. The data are presented as the mean of technical triplicates ± SD. The data are representative of three independent experiments.

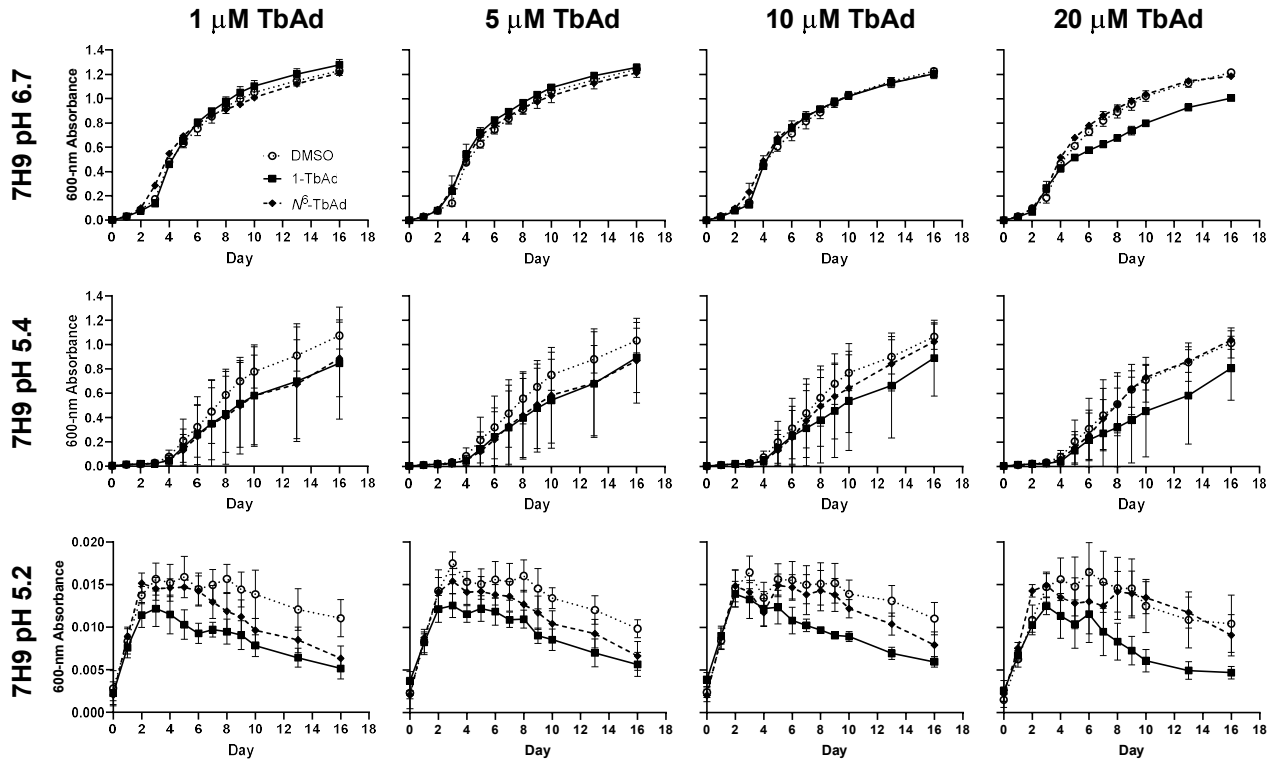

Figure 4 – Chemical complementation of *M. kansasii* with synthetic TbAd does not promote growth at any pH. (a) *M. kansasii* WT was inoculated into fresh pH-adjusted 7H9 (using HCl titration) containing the indicated concentration of TbAd isomer or DMSO, and then incubated at 37ºC in 96-well plates over 16 days. OD_{600} was measured every 1-3 days. The data are presented as the mean of technical quadruplicates ± SD.

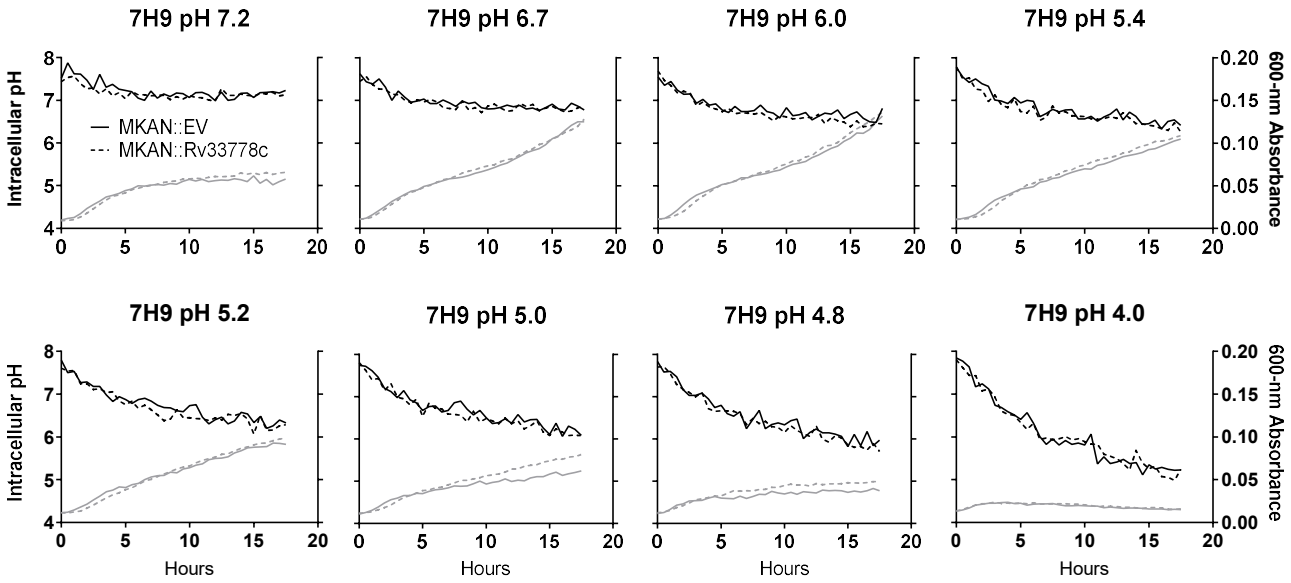

Figure 5 – 1-TbAd does not alter the intracellular pH of bacteria - *M. kansasii*::EV (MKAN::EV - solid lines) and *M. kansasii*::*Rv3377-78c* (MKAN::Rv33778c - dashed lines) cultures at equal OD_{600} were stained with CFSE, inoculated into fresh pH-adjusted 7H9 and incubated shaking at 37ºC in 96-well plates placed in the dark. Growth (grey / OD_{600} measurements) and intracellular pH (black / pH calculated from fluorescence excitation-emission ratios) readings were taken at 30-minute intervals overnight. The data are presented as the median of technical triplicates. Data are representative of 5 independent experiments.

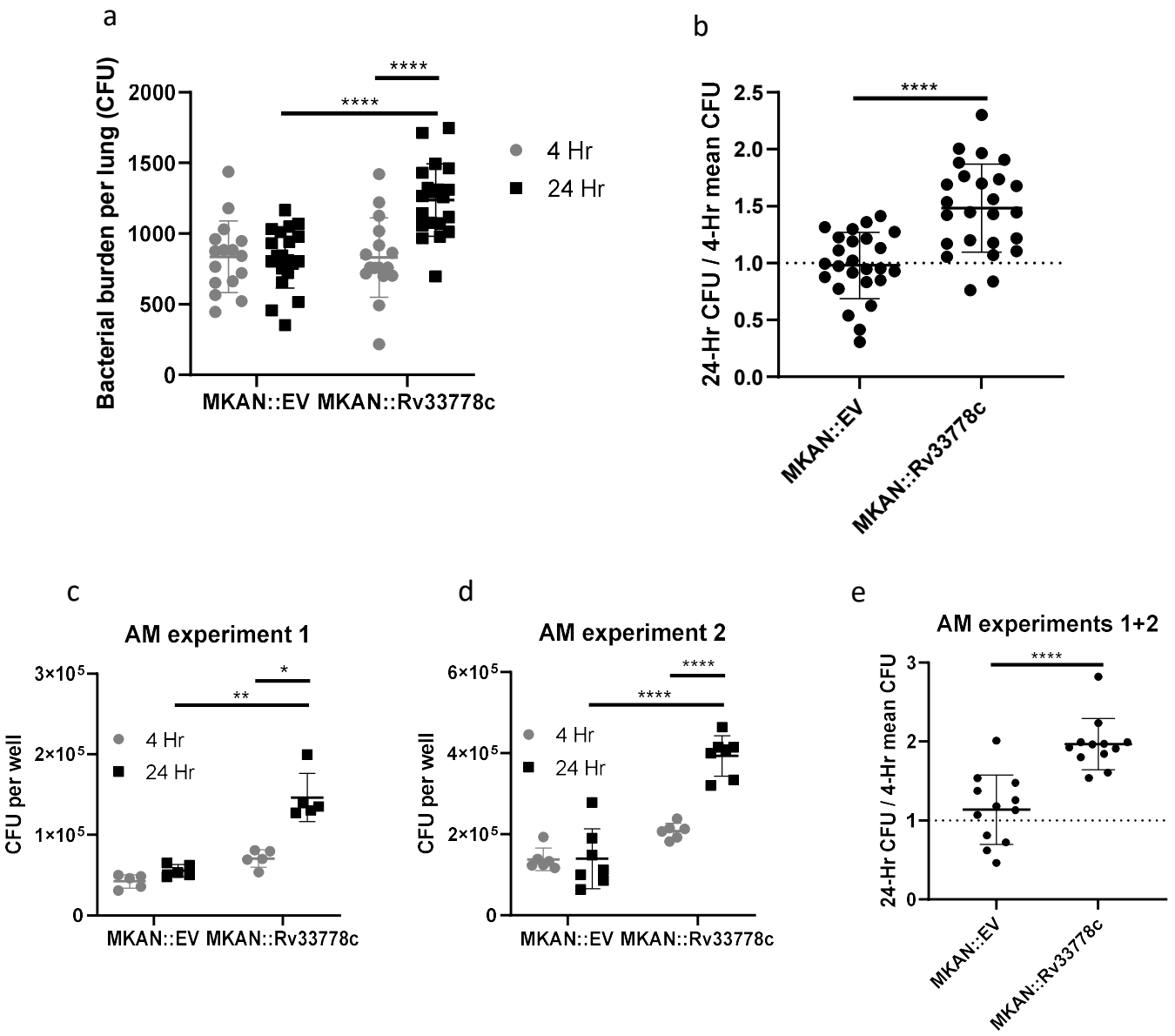

Figure 6 – 1-TbAd enhances the initial establishment of pulmonary infection. (a-b) CFUs were counted from C57Bl/6 mouse lungs isolated at 4- vs. 24-hours post aerosol infection with *M. kansasii*::EV (MKAN::EV) or *M. kansasii*::*Rv3377-78c* (MKAN::Rv33778c) (n=20 lungs/condition/time point). (a) Absolute CFU count data are pooled from two independent experiments with similar initial inoculum. (b) 24-hr CFU/mean 4-hr CFU ratio data were pooled from three independent experiments (n=21-25 lungs/condition/time point). (c-e) CFUs were counted from C57Bl/6 murine-derived AMs at 4- and 24-hours after *ex vivo M. kansasii* infection. (c-d) Absolute CFU count data from two independent experiments (N=5 and 7 replicate wells containing infected AMs, respectively, per condition per timepoint). (e) 24-hr CFU/mean 4-hr CFU ratio data pooled from two independent experiments (N=12 per condition). The data are plotted as the mean ± SD. GraphPad Prism 8.1.2 was used to perform Welch's two-tailed unpaired t-tests where *p<0.05, **p<0.01, ****p<0.0001.

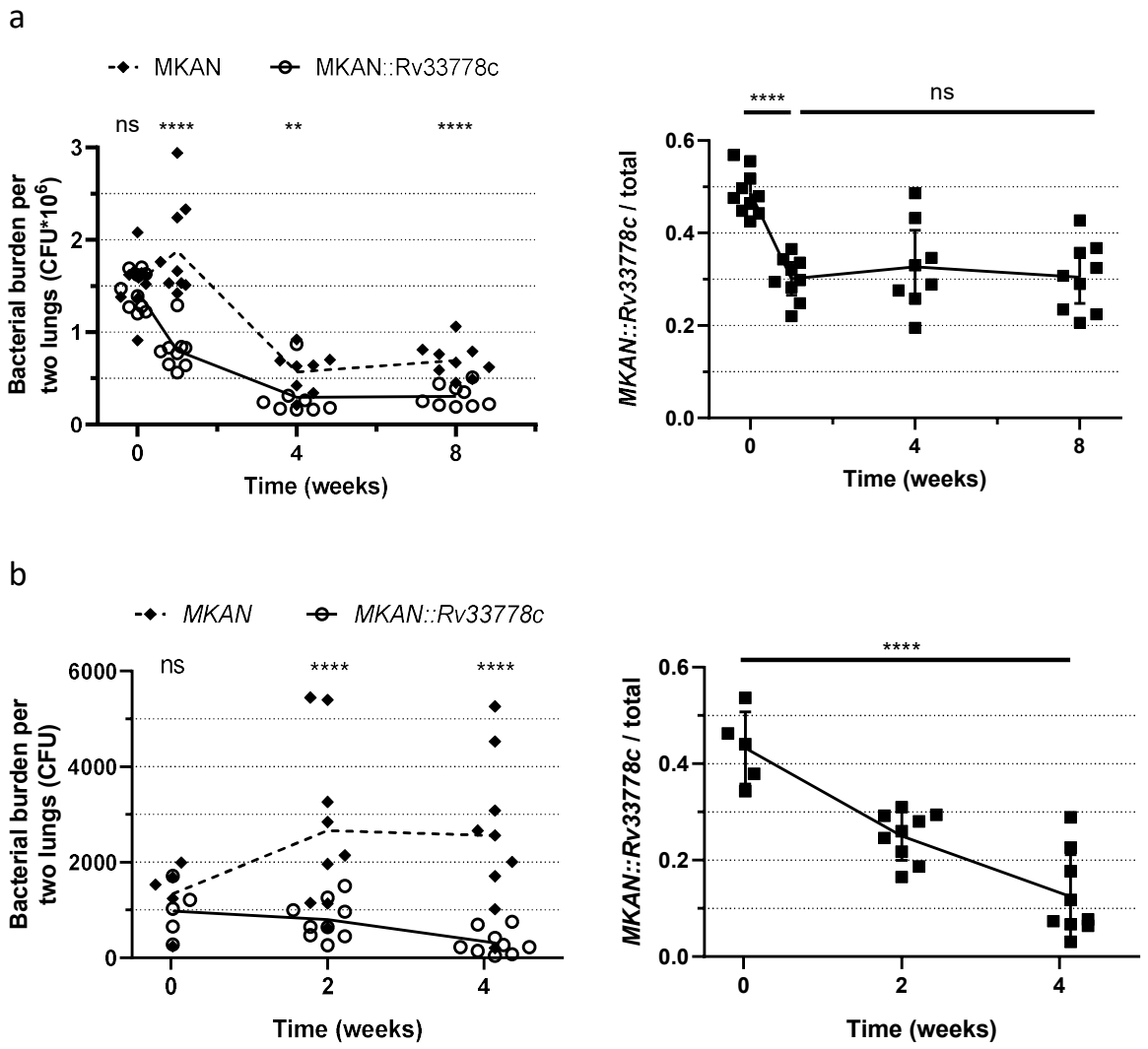

Figure 7 – 1-TbAd production hinders long-term bacterial growth. (a-b) Mixed 1:1 bacterial suspensions of WT *M. kansasii* (MKAN) and *M. kansasii::Rv3377-78c (MKAN::Rv33778c)* were used to infect (a) WT C57Bl/6 mouse lungs isolated at 1, 7, 28 and 56 days post high-dose trans-laryngeal intubation (n=8-10 lung pairs per timepoint) or (b) *Ccr2 -/-* C57Bl/6 mouse lungs isolated at 0, 14 and 29 days post aerosolization (n=5-9 lung pairs per timepoint). CFUs were counted on 7H10 plates + PANTA ± hyg50. The graphs on the right represent the proportion of *M. kansasii::Rv3377-78c* over the total number of bacteria (MKAN + MKAN::Rv33778c) per mouse per timepoint. The raw data (left) and proportions (right) are plotted as individual datapoints (± SD for proportions only). GraphPad Prism 8.1.2 was used to perform the ratio paired t-test (ratio per timepoint/left) and ordinary one-way ANOVA (proportions over time/right).